

WELDABILITY OF THE FERRITIC-MARTENSITIC STAINLESS STEELS JOINED BY FRICTION STIR WELDING

***Mustafa NURSOY**

*Abant Izzet Baysal University, Department of Mechanical Engineering, 14280, BOLU

Abstract

In this study, FSW characteristics of a ferritic-martensitic stainless steel were investigated. Gravity die cast stainless steel samples were stir welded at three different welding speeds, pre-calculated theoretically as 350, 450, and 550 rpm, with a 50-mm/min feedrate. Mechanical properties were determined by tensile tests and microhardness measurements applied on the specimens taken from the welding zones. SEM and EDS studies were performed to examine the microstructural changes and the formed phases in the weldments. As a result, FSW process was seen to be a suitable joining technique that could be applied safely for these kinds of materials. The four zones formed after the welding operation were seen to be reasonable for a sound joint.

Keywords: Friction stir welding, ferritic-martensitic stainless steel, mechanical properties.

1. Introduction

Friction Stir Welding (FSW) is a solid-phase welding process invented in 1991 at TWI (formerly The Welding Institute). Since its invention, the process has received world-wide attention, particularly for joining aluminum alloys. As shown in Fig. 1, in FSW, a cylindrical shouldered tool with a profiled probe is rotated and slowly plunged into the joint line between two pieces which are butted together [1]. Owing to the main advantages like higher mechanical strength than conventional welding because of recrystallization with fine microstructure, low distortion even in long welds, energy efficiency, and suitability for mass production; FSW obtained a large application area in joining stainless steels as well as dissimilar materials. A significant benefit of Friction Stir Welding is that it has significantly fewer process elements to control. In a Fusion weld, there are many process factors that must be controlled –such as purge gas, voltage and amperage, wire feed, travel speed, shield gas, arc gap. However, in Friction Stir Weld there are only three process variables to control: rotation speed, travel speed and pressure, all of which are easily controlled. On the other hand, the main disadvantages of the process are the need to provide a rigid support system to react against the considerable downward force exerted by the welding tool and the remaining holes at the end of each weld [2-4]. The parameters affecting the welding characteristics include the feed and rotational speed of the tool, mechanical and thermal properties of the materials to be welded, tool material, tool geometry, and welding equipment [5,6].

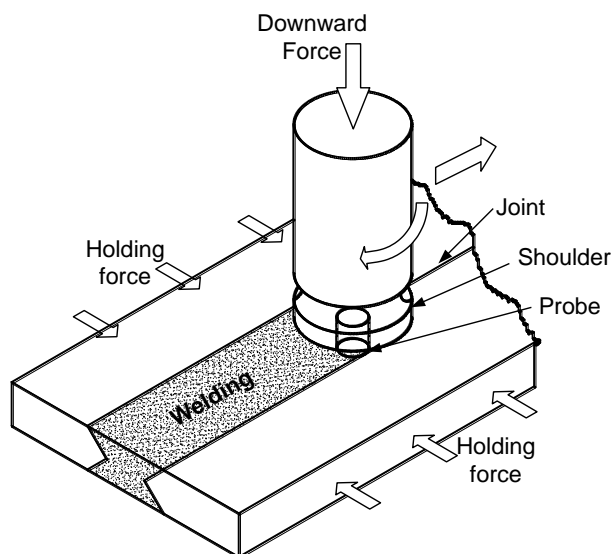


Fig.1 The mechanism of FSW

Ferritic stainless steels have certain useful corrosion properties, such as resistance to chloride stress-corrosion cracking, corrosion in oxidizing aqueous media, oxidation at high temperatures and pitting and crevice corrosion in chloride media. Susceptibility of the ferritic stainless steels to intergranular corrosion is due to chromium depletion, caused by precipitation of chromium carbides and nitrides at grain boundaries. Because of the lower solubility of carbon and nitrogen in ferrite, the synthesized zones of welds in ferritic stainless steels are heat affected zone (HAZ) and thermo-mechanically affected zone (TMAZ). With some modifications in ferritic stainless steel compositions, martensite structure is obtained to help the material have enhanced mechanical and corrosion properties. Ferritic-martensitic stainless steels have received extensive use at elevated temperatures, because of their economical combination of good mechanical and corrosion properties [7].

The purpose of this study is to examine the mechanical and microstructural properties of FSW joints made on ferritic-martensitic stainless steels. Determining the optimal operation parameters were also aimed during the experiments.

2. Experimental

Ferritic-martensitic stainless steel plates produced by gravity casting process. To prepare suitable samples, they were machined into 80×240×9 mm. The chemical composition of the material was analyzed as shown in Table 1.

Table 1. The chemical composition of the sample

	Fe	Cr	Ni	C	Si	Mn	P	S	Ti	Mo	V
%	82.03	16.79	0.302	0.071	0.049	0.207	0.176	0.162	0.004	0.048	0.020

The sample plates were tightly held by a special fixture designed and manufactured for these study (Fig.2). FSW processes were applied at three different revolutions, 350, 450, and 550 rpm, at a feed rate of 50 mm/min on a vertical milling machine. Specially designed cobalt-based tungsten carbide tips were used throughout the experiments. The diameter of the probe is 3.6 mm at the tip, and it has a tapered profile with teet grooved on. Welds have been produced by conventional FSW techniques. Each test has been conducted twice. The runs held under 1000 rpm were not included in the report because of the failure.

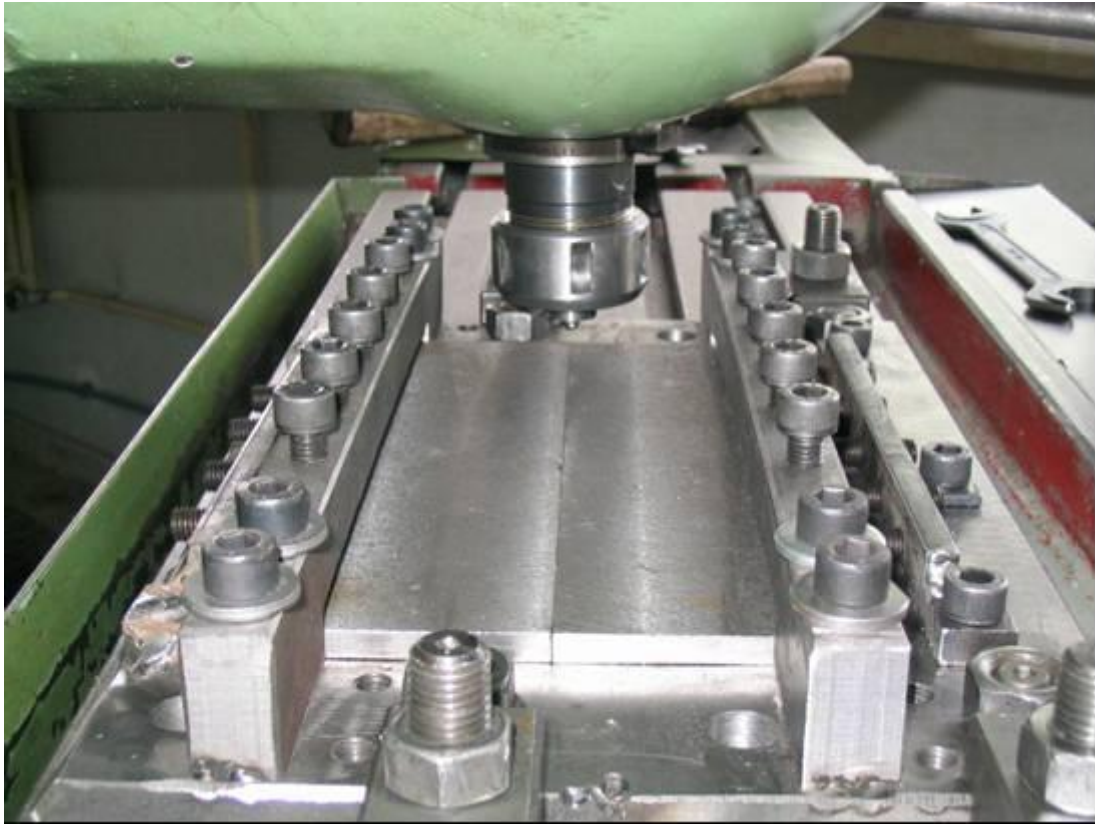


Fig.2 The fixture used for holding the parts during FSW application

Microhardness measurements and tensile tests were applied to investigate mechanical properties of the weldments. Microhardness tests were performed in atmospheric medium under 100 g, 200 g, and 300 g loads using a digital microhardness tester (Highwood HVDM3). The values in Fig.4 are the mean values. The tensile test samples were taken perpendicular to the welding direction. Visual inspection of the weld surfaces can also give significant information about the quality. Scanning electron microscopy (SEM) and energy dispersive X-Ray (EDX) analyses were performed to determine the phase formations in the structure.

3. Results and Discussions

The reason for selecting low revolutions compared to aluminum applications, which are over 1500 rpm, is to prevent the heat concentration on the tool material because of the poor conduction rate of stainless steel. The welding was successfully applied on the three different revolutions. Comparing the visual appearance and tensile test results, a revolution of 450 rpm was found to be ideal for application. The highest tensile strength among the three samples was obtained with that of 450 rpm. As the smooth welding implies, the phase distribution is homogenous, and the rupture was occurred away from the weldments, which indicates a sound seam (Fig.3). The hardness value is also highest for this sample on both horizontal and vertical directions. Main material, TMAZ, HAZ, and the weldment regions were clearly identified in the SEM micrographs cross-sectionally taken from the samples. As seen from the figures that the hardness values are varying between 300 and 350 HV in HAZ, while increasing up to 510 HV towards the junction (Fig.4). The decrease in the cases of 350 and 550 rpm can be attributed to the non-uniform distribution of the stirred ferrite and martensite phases for 350 rpm and the diminishing martensite amount for 550 rpm.

The hardness increase in the HAZ and TMAZ regions can be attributed to the formation of precipitation phases and to the changes at grain sizes. The distribution of martensite and newly formed martensite phases in these regions increases the hardness.

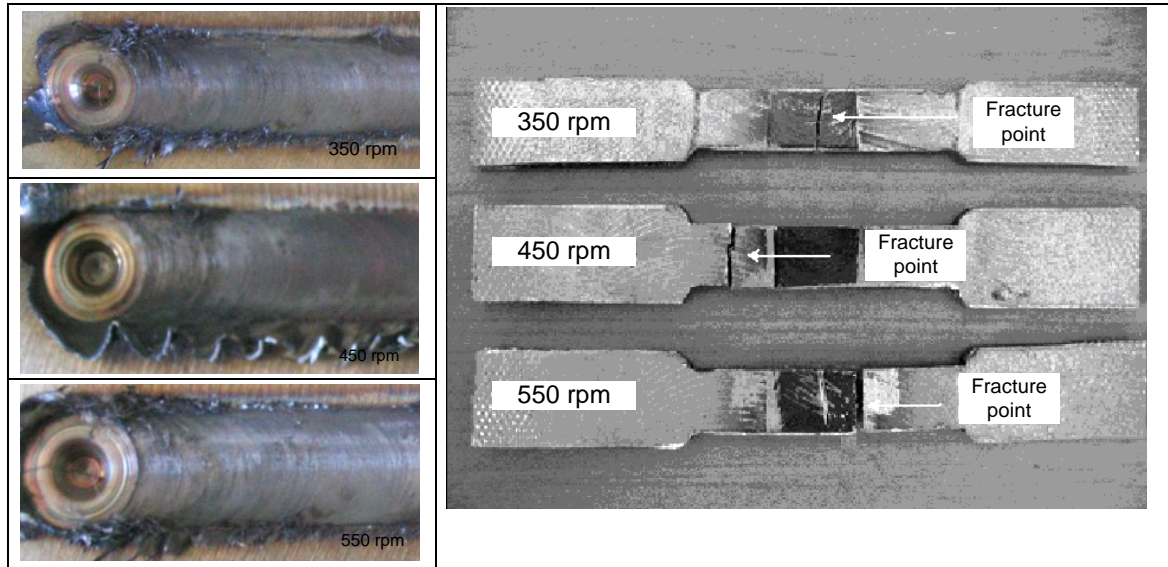


Fig.3 Physical appearances of weldments and fracture points on tensile test specimens.

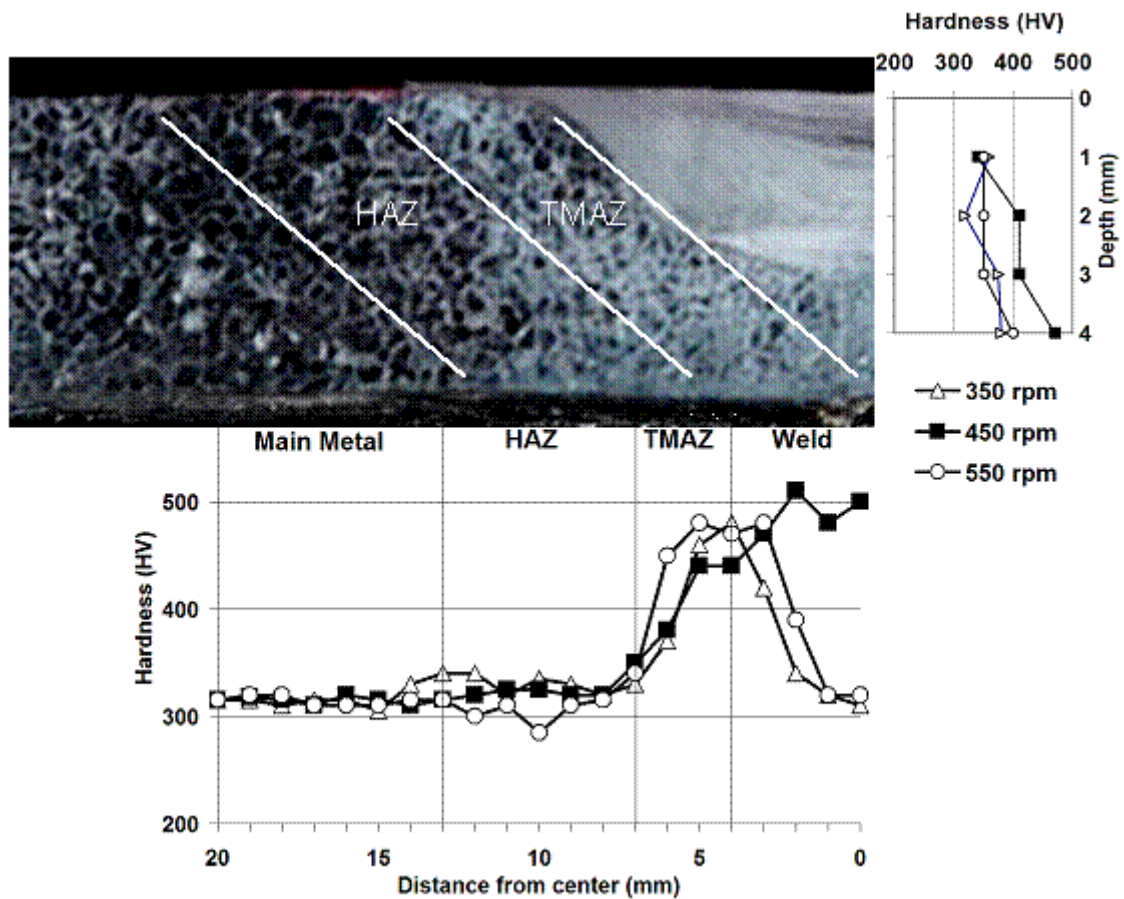


Fig.4. Horizontal and vertical hardness distributions of the weld zone.

The typical micrographs taken from the intersection areas of the weld and TMAZ show the effectiveness of the process on this materials (Fig.5). It reveals from the inspection of the micrographs that the process is successful and applicable for mass production. The transition region is smooth and free of severe plastic deformation.

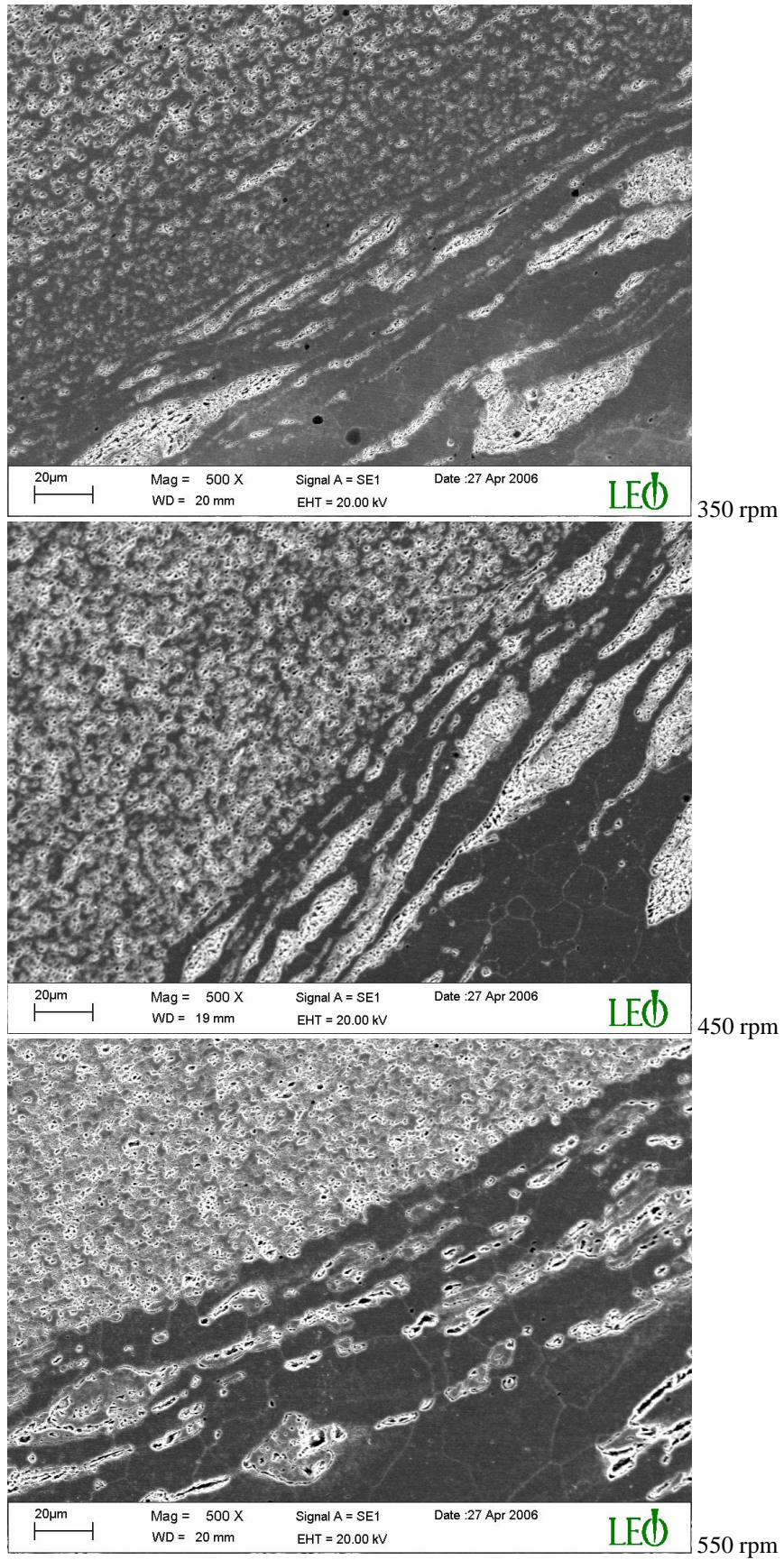


Fig.4 SEM micrographs of weldments

In 350 rpm, the forging and stirring effects of tool shoulder caused to the forced dynamic recrystallization of the weldment, which resulted finer grain sizes to 1 – 10 μm . In TMAZ, martensite and ferrite grains are coarser, 6 – 12 μm . In HAZ, no martensite deformation was observed, but the effect of heat and plastic deformation of TMAZ induced larger secondary ferrite grains, 5 – 17 μm .

In 450 rpm, the stirring is more homogenous. The size of ferrite grains are 1 – 3 μm . The carbide and martensite grains were seemed to have been crushed, and oriented to the rotational direction. In TMAZ, the ferrite and martensite grains are coarser than those of 350 rpm, 15 – 25 μm . No martensite deformation was observed in HAZ, but slight coarsening of ferrite grain sizes, 30 – 40 μm .

In 550 rpm, like in 350 and 450 rpm, dynamic recrystallization caused by stirring and forging is clear. The grains are fined to 2 – 5 μm , and the carbide and martensite grains were seemed to have been crushed and fined as well. The orientation to the rotational direction is clearly observed. Ferrite and martensite grains are coarser in TMAZ, 8 -12 μm . In HAZ, martensite was maintained with almost no deformation, and the size ferrite grains are 5 – 10 μm . Ferrite and martensite distributions are less homogenous compared to 450 rpm.

4. Conclusions

After the metallographic and mechanical examinations of the stir welded ferritic-martensitic stainless steel samples at three different welding conditions, it was concluded that:

- Using suitable tooling, ferritic-martensitic stainless steels can be FSWed without any preheating,
- About 450 rpm revolution and 50 mm/min feed rate seem to be optimal for the FSW of these materials,
- Although solid state processes are prone to distortions and deformational faults, almost no harmful structural deformation are recorded. The process was quite stable.

References

1. Friction Stir Welding, <http://www.twi.co.uk/> (Assessed on Feb 1, 2008)
2. Hatsukade Y, Takahashi T, Yasui T, Tsubaki M, Fukumono M, Tanaka S. “Study on nondestructive inspection using HTS-SQUID for friction stir welding between dissimilar metals”. *Physica C*, v. 463–465, s. 1038–1042, 2007.
3. Mishra RS, Ma ZY, “Friction stir welding and processing”, *Materials Science and Engineering: R: Reports*, v 50, p.1-78, 2005.
4. Uzun H, Dalle Donne C, Argagnotto A, Ghidini T, Gambaro C. “Friction stir welding of dissimilar Al 6013-T4 To X5CrNi18-10 stainless steel”, *Materials & Design*, v. 26, p. 41-46, 2005.
5. Reynolds AP, Tang W, Gnaupel-Herold T, Prask H, “Structure, properties, and residual stress of 304L stainless steel friction stir welds”, *Scripta Materialia*, v.48, p.1289- 1294, 2003.
6. Park SHC, Sato YS, Kokawa H, Okamoto K, Hirano S, Inagaki M, “Corrosion resistance of friction stir welded 304 stainless steel” , *Scripta Materialia*, v. 51, p.101-105, 2004.
7. Marinelli MC, Degallaix S, Alvarez-Armas I, “Dislocation structure developed in the austenitic-phase of SAF 2507 duplex stainless steel”, *Materials Science and Engineering:A*, v. 435-436, p. 305-308, 2006
8. Sato YS, Nelson TW, Sterling CJ, Steel RJ, Pettersson CO. “Microstructure and mechanical properties of friction stir welded SAF 2507 super duplex stainless steel”. *Materials Science and Engineering:A* v. 397: p. 376–384, 2005